Validation of a CT-guided intervention robot for biopsy and radiofrequency ablation: experimental study with an abdominal phantom

Hyung Jin Won
Namkug Kim
Guk Bae Kim
Joon Beom Seo
Hongho Kim

PURPOSE
We aimed to evaluate the accuracy of a needle-placement robot for biopsy and radiofrequency ablation on an abdominal phantom.

METHODS
A master-slave robotic system has been developed that includes a needle-path planning system and a needle-inserting robot arm with computed tomography (CT) and CT fluoroscopy guidance. For evaluation of its accuracy in needle placement, a commercially available abdominal phantom (Model 057A; CIRS Inc.) was used. The liver part of the phantom contains multiple spherical simulated tumors of three different size spheres. Various needle insertion trials were performed in the transverse plane and caudocranial plane two nodule sizes (10 mm and 20 mm in diameter) to test the reliability of this robot. To assess accuracy, a CT scan was performed after each trial with the needle *in situ*.

RESULTS
The overall error was 2 mm (0–2.6 mm), which was calculated as the distance from the planned trajectory before insertion to the actual needle trajectory after insertion. The standard deviations of the insertions on two nodules (10 mm and 20 mm in diameter) were 0.5 mm and 0.2 mm, respectively.

CONCLUSION
The CT-compatible needle placement robot for biopsy and radiofrequency ablation shows relatively acceptable accuracy and could be used for radiofrequency ablation of nodules ≥10 mm under CT fluoroscopy guidance.

C omputed tomography (CT)-guided interventions such as biopsy, catheter drainage, and radiofrequency ablation are widely used as minimally invasive diagnostic and therapeutic procedures. The use of CT fluoroscopy helps to reduce the procedure time, patient radiation dose, and complications, particularly in risky locations near large vessels and the gastrointestinal tract. Reported success rates of conventional CT and CT fluoroscopy-guided biopsies range from 90%–100% and 83%–100%, respectively (1–3). However, CT-guided interventions are time-consuming procedures and should be performed by experienced interventional radiologists. In addition, significant radiation exposures occur to medical personnel when CT fluoroscopic guidance is used.

Recently, development of the robotic surgery platform has provided a tool that can overcome many of the limitations of conventional surgery. Augmented dexterity enabled by the endowristed movements, software filtration of the surgeon's movements, and enhanced vision provided by the stereoscopic camera combine to allow steady and careful dissection and prompt and precise suturing (4, 5). These advantages of the robotic system can also enable accurate targeting with diverse angulation of the robotic arm in CT-guided biopsy and tumor ablation. Furthermore, robotic intervention can potentially decrease procedure time and radiation exposure to both patients and doctors (6).

We developed a robotic system with path-planning and needle-placement functions under CT guidance. The purpose of this experiment was to assess the stability and accuracy of our CT-guided intervention robot using an abdominal phantom.

Methods

Robot system

The interventional robotic system used in this study is a master-slave type robotic system for CT-guided needle intervention jointly developed by our hospital and a manufacturer (Fig. 1).

From the Departments of Radiology (H.J.W. ✉ *hjwon@amc.seoul.kr*, N.K., J.B.S.) and Convergence Medicine (N.K., G.B.K.), University of Ulsan College of Medicine, Asan Medical Center, Seoul, Korea; Corporate Technology Institute (H.K.), Hyundai Heavy Industries Co. Ltd., Ulsan, Korea.
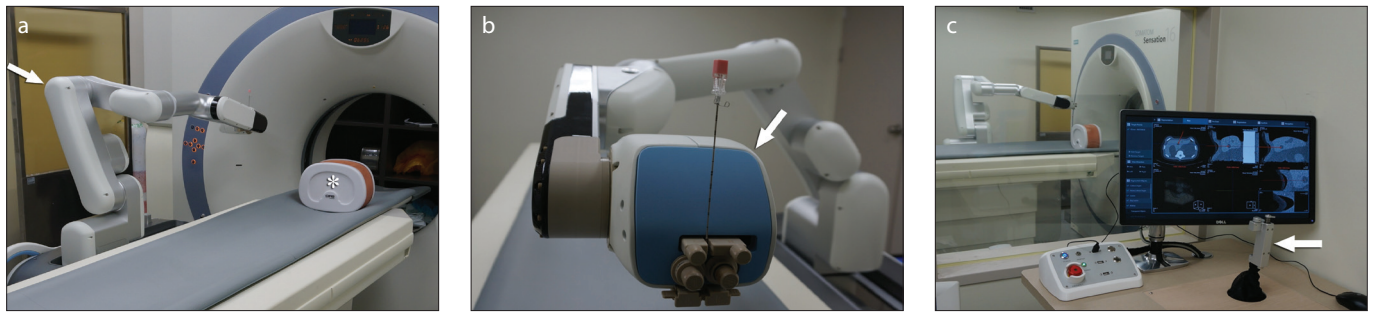
Figure 1. a–c. CT-guided needle-placement robot. Panel **(a)** shows the robot *(white arrow)* placed alongside a CT scanner with an abdominal phantom *(asterisk)* on it. End-effector holding a biopsy needle (**b**, *white arrow*), and a master console with joystick (**c**, *white arrow*) are seen.

The robot system is mainly composed of three sub-systems (Fig. 2). Master console is an integrated user interface for the purpose of manipulating and monitoring the whole system. Slave robot has a five-axis robot arm, an end-effector, and a motor controller. The end-effector is attached to the distal end of the robot arm for the installation and insertion of needle. Localizer is temporarily used for CT-robot spatial registration when the slave robot is initially set up on the floor beside the CT table or moved.

The slave robot has dimensions of 1.1 m × 0.47 m × 1.9 m (length × width × height), with the robot arm positioned in the ready condition. The weight of the slave robot is about 250 kg. The slave robot has one swivel caster wheel in the rear and two front fixed caster wheels. It is also fixed on the floor through a lifting system. Master console has dimensions of 0.8 m × 0.73 m × 1.8 m (length × width × height) including a 23-inch monitor. The weight of the master console is about 200 kg. The master console has four swivel caster wheels.

The accuracy of identifying the relationship between CT image space and robot space is assumed to be the most important in needle insertion accuracy of inter-
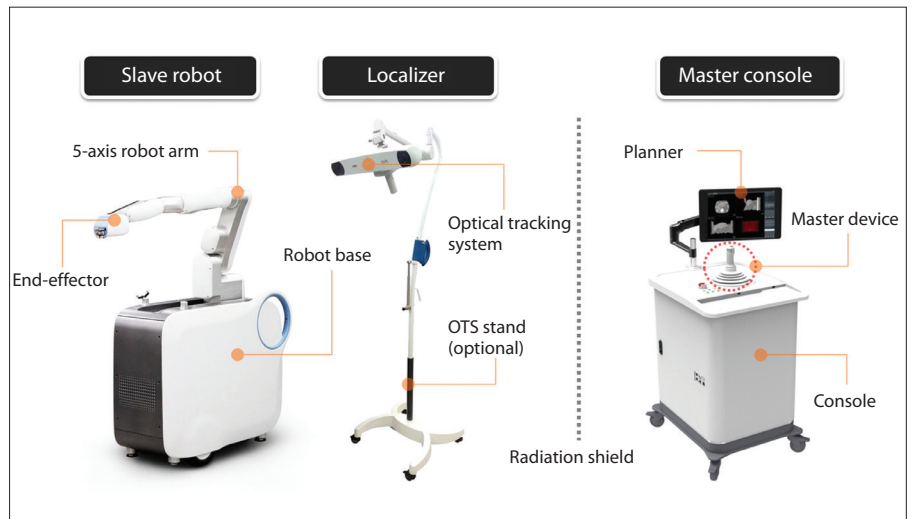

Figure 2. Components of interventional robotic system.

ventional robotic system. Optical tracking system (Passive Polaris Spectra®; Northern Digital Inc.) used in the robotic system is one of the robust and easy-to-use external tracking systems. According to the manufacturer, it has 0.35 mm RMS (root mean square) error in three-dimensional (3D) position tracking. A custom-designed registration jig is also used for the spatial registration and its validation (Fig. 3). The registration jig has several sets of retro-reflective ball markers and acrylonitrile-butadiene-styrene plastic rods. Position data of the ball markers in CT image space and optical tracking system space determines a 4×4 homogeneous transformation matrix. Simultaneous tracking robot-side optical tool attached to the robot base and the ball markers on the registration jig leads to the relationship between CT image space and robot space.

For needle path planning, CT scan data is transferred from CT console to the planner software through a network. Multiplanar reconstruction view is rendered as shown in

Fig. 4. Then, needle path is initiated by user's selection of a target position. User can modify the needle path by changing the position of target or entry.

The robotic system allows a conventional biopsy needle or radiofrequency ablation needle to be used. After the planned needle path is confirmed by user, a few sterilized parts are installed on the end-effector manually. Then, the robot arm waits for a manual input to move toward a target pose. When the initial movement of the robot arm is completed, communication between master device and slave robot arm is opened in a real-time network protocol. Real-time operating platform is built in the robotic system. The robot arm can be manipulated by user's control of the master device. In this study, however, the master device was used only for needle insertion because position and orientation of the robot arm was fixed after the initial movement in each test. Additional manipulation of the robot arm based on visual feedback is excluded from the system accuracy in this study.

Main points

- Robotic system for CT-guided biopsy and tumor ablation may enable accurate targeting as well as decrease procedure time and radiation exposure to both patients and doctors.

- The reliability and accuracy of our CT-guided intervention robot were validated with an abdominal phantom.

- The CT-compatible needle placement robot for biopsy and radiofrequency ablation shows relatively acceptable accuracy and could be used for radiofrequency ablation of 1 cm-sized nodules under CT fluoroscopy guidance.
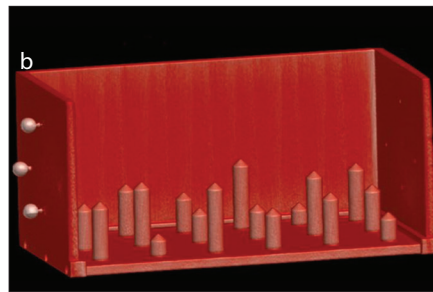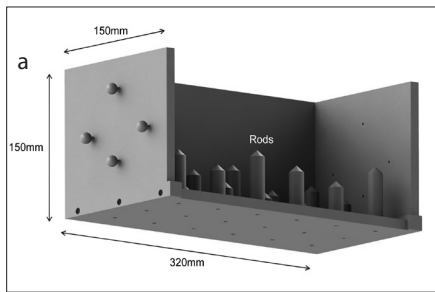
Figure 3. a, b. Custom-designed registration jig; computer-aided design (CAD) data **(a)** and 3D reconstruction of CT scan **(b)**.
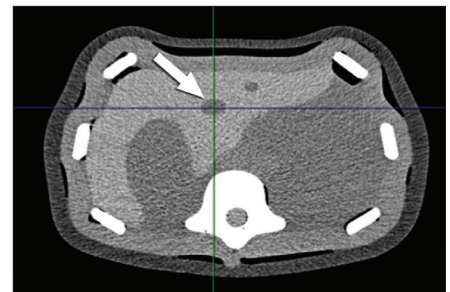

Figure 5. Abdominal phantom. CT scan showing a target nodule *(white arrow)* in the left lobe of the simulated liver.
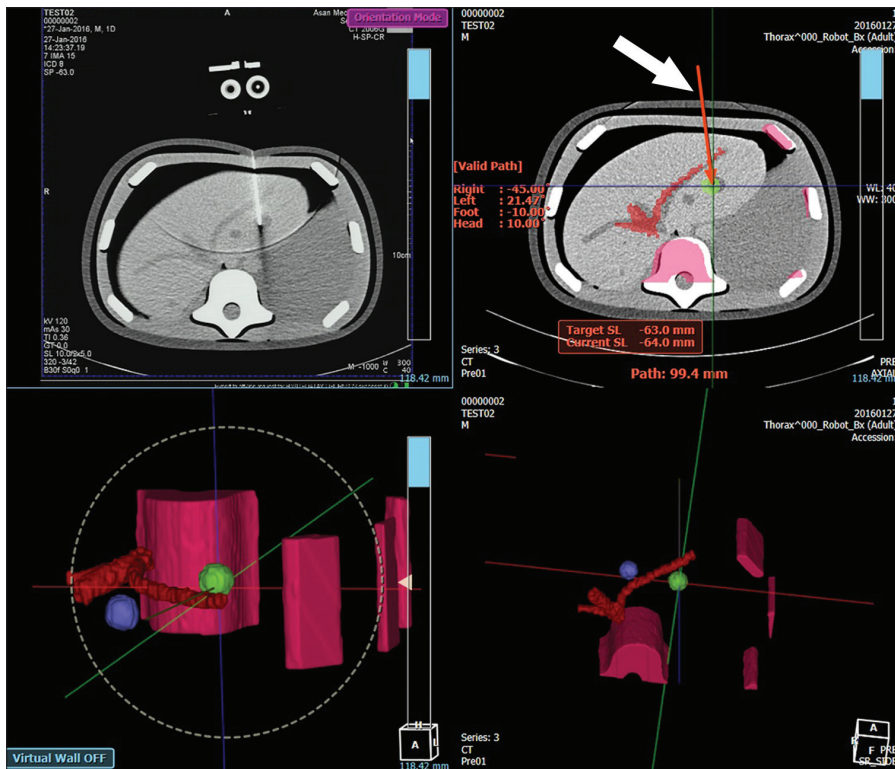

Figure 4. Screenshot of the path-planning user interface of CT-guided needle placement robot. The top left panel is a CT fluoroscopy image. The top right panel is a planning screen. Solid red line *(white arrow)* represents the needle path that is located along the viewed slice. It changes to a dotted line when the path crosses two slices or more. The bottom panels are 3D rendering of the planned needle path.

Table. Summary of the test protocol

Nodule size (mm)	Insertion angles (°)			
	0°	15°	30°	CC 20°
10 mm	7	2	2	2
20 mm	7	2	2	2
CC, caudocranial.				

Abdominal phantom

A commercially available 3D abdominal phantom (Model 057A; CIRS Inc.) (Fig. 5) was used (7). The phantom is representative of a small adult abdomen and can be imaged by CT, magnetic resonance imaging, and ultrasonography. It simulates the abdomen from the thoracic (T9/T10) to the lumbar vertebrae (L2/L3). Internal structures include the liver, hepatic vessels, two partial kidneys, and a partial lung. The simulated liver has six lesions in a range of sizes (small, medium, and large lesions; two of each size).

Test protocol

The phantom was scanned by a Sensation 16-row multidetector CT (Siemens Healthcare) for baseline imaging. The scanning parameters were as follows: slice thickness 1 mm, 120 kV, 200 mAs. The liver part of the phantom contains multiple spherical simulated tumors of three different size spheres. A Westcott fine needle aspiration biopsy needle, 20 gauge × 7 inches (BD Medical), was used. Various needle insertion trials with two nodule sizes (10 mm and 20 mm in diameter) and four insertion angles (0°, 15°, 30° in the transverse plane, and 20° in the caudocranial plane) were performed twice per parameter. The two nodules were located in segment IV according to Couinaud's classification. In addition, five insertions on each nodule with 0° in the transverse plane were added to evaluate the precision and reliability of this robot (Table).

Assessment of accuracy

To assess accuracy, the CT scan was repeated with the same scan parameters after each trial with the needle *in situ*. Using intrinsic planning software system, the center of the target nodule was marked on multiplanar reformation view and recorded on the 3D space. Targeting errors were measured by obtaining the minimum distance between the nodule center and the biopsy needle tip (Fig. 6).

Statistical analysis

Accuracy measurement and procedure time were statistically evaluated with STATA software version 12 (StataCorp, LLC). Each measurement was tested by Shapiro-Wilk normality test. For nonparametric comparison, we performed Wilcoxon rank sum test for nodule sizes and Kruskal-Wallis test for insertion angles.

Results

The overall targeting error measured from the center of the nodule to the needle tip
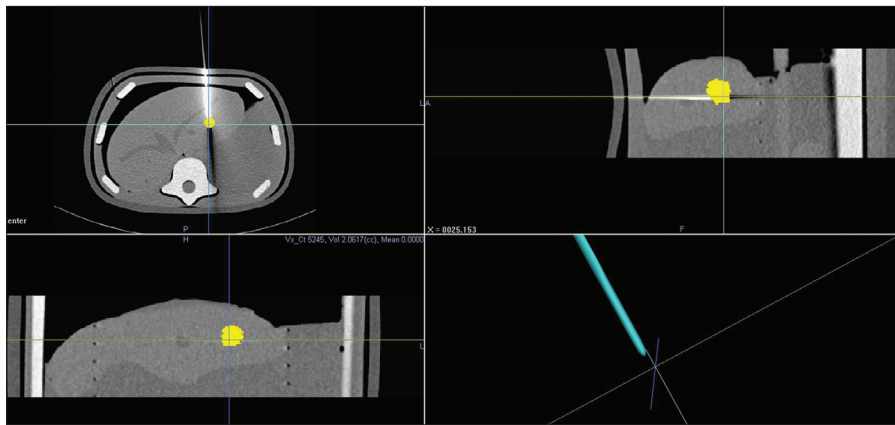
Figure 6. Measurement of targeting accuracy. Targeting errors were measured by obtaining the distance between the nodule center and the biopsy needle tip. The lower right image shows the nodule center (intersection of lines) and the needle tip.

was 2 mm (0–2.6 mm). Targeting error was not significantly different between nodule sizes of 10 mm and 20 mm. Targeting errors were larger for insertion angles of 0° ($P = 0.011$) and caudocranial 20° ($P = 0.007$). In order to evaluate the precision and robustness, seven trials were performed on two nodules (10 mm and 20 mm in diameter) with vertical (0°) insertions. The standard deviations were 0.5 mm for 10 mm nodule and 0.2 mm for 20 mm nodule. The median procedure time measured from pre-positioning to release of the needle was 31 s (18–54 s).

Discussion

The overall error of our robotic system, which corresponds to the distance between the center of the target nodule and the needle tip, was below 3 mm. Pereles et al. (8) performed experimental phantom study comparing accuracy of laser-guided and freehand CT biopsy. They reported that mean error with freehand technique was 10.58 mm (standard error [SE], 0.82 mm) and mean error with laser guidance was 5.01 mm (SE, 0.41 mm). Our results are more accurate than their laser-guided as well as freehand data. This level of targeting accuracy (less than 3 mm) can be used in clinical practice with human supervision after undergoing further durability and safety tests in animal experiments and clinical trials. Mean targeting errors were significantly larger for insertion angles of 0° and caudocranial 20°. Inadvertent bending and deviation of the biopsy needle in penetrating the simulated skin part of the phantom might be the source of variation according to insertion angles.

Challenges of conventional CT-guided procedures include limited entry plane and angle, long procedure time, radiation exposure, and steep learning curve. Possible advantages of a robotic system could be more accurate targeting with diverse angulation of the robotic arm in CT-guided biopsy and tumor ablation. The robot arm is free from the inherent instability and tremor of human hands and can execute pre-planned movements with precision. It can also provide an increased degree of freedom in intervention planning including caudo-cranial (i.e., z-axis) angulation, thus being more flexible in avoiding high-risk organs. Other benefits would be reduced procedure time and radiation exposure to both patients and doctors. The median procedure time of our system was 31 s. Although an objective comparison with conventional human procedure is not easy, this is an acceptable performance for a work-in-progress system. Our robotic system might also be transformed into an educational device for CT-guided intervention. On the other hand, the operators of a robotic system could not have tactile feeling with needle insertion that frequently gives them feedback regarding positioning in the right tissue.

There are two robotic positioning systems for CT-guided interventions currently in the market; Maxio (Perfint Healthcare) and iSYS1 (Medizintechnik). Maxio's mean tip-to-target distance, which corresponds to overall error of our system, was 6.5±2.5 mm (9). Our system has shown improved accuracy; overall error was 2 mm. Exclusion of human hand instabilities during needle placement process might have contributed to our enhanced accuracy, as well as robot's targeting performance. Abdullah et al. (6) performed radiofrequency and microwave ablation of liver tumors on 20 patients (40 lesions) using Maxio and reported high performance level and safety. But there was no statistically significant dose reduction in comparison with the conventional method. Also, Maxio has the robot fixed to its stand on the floor, so it is not easy to insert the needle under CT-fluoroscopy monitoring, which is a limitation of this system. Meanwhile, iSYS1 robotic system was designed to be mounted on the CT table, so it allows needle positioning and insertion inside the gantry under fluoroscopy. An experimental study with torso phantom was performed with the iSYS1 system and the Euclidean distance between the actual 17G biopsy needle tip and the copper wire target was 2.3±0.8 mm (range, 0.9–3.7 mm) (10). In contrast, our robotic system is equipped with remote-controlled needle insertion function. Thus, real-time monitoring of needle insertion is possible without exposing the physician to radiation.

After the performance test, we found some problems to be resolved in our robot. First, the needle-driving power of the end-effector was sometimes not strong enough to overcome the harder part of the abdominal phantom. A powerful end-effector mechanism that can prevent inadvertent deviation of the needle needs to be developed. Second, the user interface of the master console requires further refinement including more intuitive manipulation for inexperienced users. Third, safety measures should be reinforced before proceeding to animal experiments and clinical trials. Currently, our robot is equipped with a "danger zone" warning system. Users can preset dangerous organs such as the heart, great vessels, and bowels as danger zone, i.e., no-fly zone. When the needle approaches the danger zone, an alarm will sound. If the needle continues to reach the danger zone, it will automatically stop. Tests of safety measures should be performed in various simulated emergencies, including abrupt movement of the patients. Lastly, an inherent limitation of our phantom experiment is overcoming respiratory movement in clinical setting. In case of radiofrequency ablation, general anesthesia with temporary pause of ventilator in end-expiratory phase can be an effective motion control measure. However, effective monitoring and gating of respiratory movement is needed in order to perform other interventional procedures in patients under sedation. Another limitation of our experimental study is the small sample size of each test protocol

(n=2), which limits statistical comparison of groups. Further experiments with phantoms and animals need to be performed before proceeding into clinical trials.

In conclusion, our CT-compatible needle placement robot for biopsy and radiofrequency ablation shows relatively acceptable degree of accuracy, and it may be used for targeting liver nodules as small as 1 cm in diameter under the supervision of an interventional radiologist.

Conflict of interest disclosure

Hongho Kim is an employee of Hyundai Heavy Industries, Co., Ltd. Joon Beom Seo has received a grant (#10041618) from the Ministry of Trade, Industry, and Energy, Korea. No conflicts of interest were declared for the remaining authors.

References

1. Carlson SK, Bender CE, Classic KL, et al. Benefits and safety of CT fluoroscopy in interventional radiologic procedures. Radiology 2001; 219:515–520. [CrossRef]
2. Silverman SG, Tuncali K, Adams DF, et al. CT fluoroscopy-guided abdominal interventions: techniques, results, and radiation exposure. Radiology 1999; 212:673–681. [CrossRef]
3. Thanos L, Zormpala A, Papaioannou G, et al. Safety and efficacy of percutaneous CT-guided liver biopsy using an 18-gauge automated needle. Eur J Intern Med 2005; 16:571–574. [CrossRef]
4. Giulianotti PC, Coratti A, Angelini M, et al. Robotics in general surgery: personal experience in a large community hospital. Arch Surg 2003; 138:777–784. [CrossRef]
5. Milone L, Daskalaki D, Fernandes E, Damoli I, Giulianotti PC. State of the art in robotic hepatobiliary surgery. World J Surg 2013; 37:2747–2755. [CrossRef]
6. Abdullah BJ, Yeong CH, Goh KL, et al. Robotic-assisted thermal ablation of liver tumours. Eur Radiol 2015; 25:246–257. [CrossRef]
7. Triple modality 3D abdominal phantom, Model 057A. Computerized Imaging Reference Systems, Inc., 2013; cited 22 January 2016. Available at: http://www.cirsinc.com/products/all/65/triple-modality-3d-abdominal-phantom/.
8. Pereles FS, Baker M, Baldwin R, Krupinski E, Unger EC. Accuracy of CT biopsy: laser guidance versus conventional freehand techniques. Acad Radiol 1998; 5:766–770. [CrossRef]
9. Koethe Y, Xu S, Velusamy G, Wood BJ, Venkatesan AM. Accuracy and efficacy of percutaneous biopsy and ablation using robotic assistance under computed tomography guidance: a phantom study. Eur Radiol 2014; 24:723–730. [CrossRef]
10. Kettenbach J, Kara L, Toporek G, Fuerst M, Kronreif G. A robotic needle-positioning and guidance system for CT-guided puncture: ex vivo results. Minim Invasive Ther Allied Technol 2014; 23:271–278. [CrossRef]